Supporting Information

for

Long-distance transfer of plasmonic hot electrons across Au-Pt porous interface for the hydrogen evolution reaction

Chang Xia,[a] Peng Fei Gao,[b] Wei He,[b] Ye Wang,[a] Chun Hong Li,[b] Hong Yan Zou,[b] Yuan Fang Li,[a] * and Cheng Zhi Huang,[b] **

[a] Key Laboratory of Luminescence Analysis and Molecular Sensing (Southwest University), Ministry of Education, College of Chemistry and Chemical Engineering, Southwest University, Chongqing 400715, P. R. China.

[b] Key Laboratory of Luminescent and Real-Time Analytical System (Southwest University), Chongqing Science and Technology Bureau, College of Pharmaceutical Sciences, Southwest University, Chongqing 400715, P. R. China.

1. Experimental procedures

1.1 Materials

Chloroauric acid trihydrate ($HAuCl_4 \cdot 3H_2O$, >99%) was purchased from Sinopharm Chemical Reagent Co., Ltd. (Shanghai, China). Cetyltrimethylammonium bromide (CTAB, >99%), cetyltrimethylammonium chloride (CTAC, 97%), sodium borohydride ($NaBH_4$, 99%), silver nitrate ($AgNO_3$, 99.8%), ascorbic acid (AA, >99%) and chloroplatinic acid (H_2PtCl_6, 99.95%) were obtained from Aladdin Biochemical Technology Co., Ltd. (Shanghai, China). 3-mercaptopropyltrimethoxysilane were obtained from Macklin Biochemical Technology Co., Ltd. (Shanghai, China). Methanol, sodium hydroxide (NaOH) and hydrochloric Acid (HCl) were purchased form Chuandong Chemical Co., Ltd. (Chongqing, China). All reagents were used as received. All solutions were prepared using ultrapure water (18.2 MΩ) from a Milli-Q system (Millipore, Bedford, MA, USA).

1.2 Apparatus

Scanning electron microscopy (SEM) images were collected with a S-4800 field-emission SEM instrument (Hitachi, Japan). Transmission electron microscopy (TEM) characterization was performed on a FEI Tecnai G2 F20 TEM instrument (FEI, America). Extinction spectra were obtained with a U-3010 spectrometer (Hitachi, Japan). Plasmon resonance light scattering (PRLS) images were real-time captured by a BX73 optical microscope (Olympus, Japan) focused through a U-DCW NA 1.2-1.4 high numerical dark field condenser, in which a 100 W halogen lamp was mounted on as light source. The scattered light was collected using a 100×oil immersion objective and the images were taken using a DP72 single chip true-color charge-coupled device (CCD)

camera (Olympus, Japan). A monochromator was equipped with a SR303i-B spectrograph (Andor, England) and the recording was carried out using a DU970P-BVF CCD spectrometer (Andor, England) to obtain the scattering spectra. The PRLS images were analyzed with Image-Pro Plus 6.0 (IPP) software (Media Cybernetics, USA). The FDTD simulations were performed on FDTD solutions (Lumerical Solutions, Inc., Vancouver, Canada). Ultrafast Transient Absorption (TA) Spectra were recorded by the laser source of the homemade spectroscopy with a commercial femtosecond amplifier laser system (35fs, 1 kHz, 800nm, Spitfire Ace, Spectra Physics). All electrochemical measurements were carried out using a CHI 900D instrument (Chenhua, China).

1.3 Synthesis of Au NSs

Preparation of gold seeds: Au NSs were produced by the previously reported seed-mediated growth method.[1] Briefly, 0.103 mL of $HAuCl_4$ solution (1% w/w) was first mixed with a 9.9 mL of 0.1 M CTAB solution, followed by the quickly injection of a freshly-prepared, ice-cold $NaBH_4$ solution (0.01 M, 0.60 mL) under vigorous stirring for 2 min. The resultant solution was aged for 3 h at room temperature before use.

Growth of the small Au NSs: The growth solution was prepared by sequentially mixing CTAB (0.1 M, 4.875 mL), $HAuCl_4$ (1% w/w, 0.817 mL), AA (0.1 M, 7.5 mL), and water (95 mL). Then, 0.06 mL of the as-prepared seed solution was injected into the growth solution. The reaction mixture was gently shaken and then left undisturbed for 12 h at room temperature. The small Au NS sample was concentrated by four times for further use.

Growth of the Large Au Nanopolyhedrons: The Au nanopolyhedrons were grown by the seed-mediated method using the small Au NSs as seeds. Typically, a 4 mL seed solution was added into a CTAC solution (0.025 M, 30 mL). 0.75 mL of 0.1 M AA and

0.613 mL of $HAuCl_4$ (1% w/w) was then added into the mixture solution followed by placing in an air-bath shaker (45 °C, 160 revolutions per minute) for 3 h. The obtained Au nanopolyhedrons were centrifuged and redispersed in a CTAB solution (0.02 M, 30 mL).

Preparation of the Large Au NSs: The large Au NSs were prepared by oxidizing the obtained Au nanopolyhedrons with $HAuCl_4$. A 30 mL Au nanopolyhedrons solutions were mixed with a $HAuCl_4$ solution (1% w/w, 0.082 mL). The mixture was kept in the air-bath shaker (45 °C, 160 rpm) for 2 h. The obtained Au NSs were stored in 4 °C refrigerator.

1.4 Characterization of Au@Pt NSs

In order to obtain the synthesized nanoparticles for TEM and SEM characterization, then Au NSs were attached to previously cleaned and 3-mercaptopropyltrimethoxysilane-treated glass slides for 4 h, then washed thoroughly with ultrapure water. Because of electrostatic attraction, the Au NSs were fixed on glass slides with a relative high density. After e^-_{ph}-reduction of $PtCl_6^{2-}$ to Pt (0) atoms, these core-shell nanoparticles were removed from the glass via ultrasonic treatment in 3.0 mL of ultrapure water for 30 min. The nanoparticles were centrifuged (9000 rpm, 5 min), washed with ultrapure water, and resuspended in 500 μL of aqueous solution for TEM and SEM characterization.

1.5 Real time monitoring through single-particle scattering measurements

First, the Au NSs were immobilized on the glass slides with a suitable density. To real-time monitor the evolution of plasmon driven reduction, a homemade microfluidic cell was utilized. A fixed observation window containing green scattering light Au NSs

was selected for real-time observation. In a typical process, 200 μL of H_2PtCl_6 aqueous solution (0.5 mM, pH=7) was added into the flow cell. The 100 W halogen lamp of dark field microscopy was employed to light irradiation with a power source of 24 mW cm^{-2}. Next, consecutive DFM images in the same area were recorded with BX73 optical microscopy at a rate of 5 minutes 1 frame. For the different influences of e_{ph}^--driven chemical reduction, scattering measurements were also proceeded following similar procedure except controlling different variable factors. A xenon lamp equipped with a series of band-pass filters (λ 460±15, 525±10, and 620±15 nm, respectively, with the emission power adjusted to 24 mW cm^{-2}) were employed to investigate the dependence of the illumination wavelength.

1.6 FDTD simulations

A wavelength range from 400 to 650 nm was radiated into a box containing a model of a nanostructure (dielectric functions of Au were taken from the experimental data conducted by palik). The surrounding medium inside the box was divided into the meshes of 0.5 nm, and its refractive index was set to be 1.33 for water. The diameters in the model were used for the calculations based on the TEM image.

1.7 Ultrafast TA spectra

The laser source of the homemade spectroscopy setup is a commercial femtosecond amplifier laser system (35fs, 1 kHz, 800nm, Spitfire Ace, Spectra Physics). The output pulse was split into two beams. The first beam was used to pump an optical parametric amplifier (TOPAS prime, Spectra Physics) to generate the excitation pulse. The second beam with weaker energy was focused into a continuous moving CaF2 plate (4 mm thickness) to generate a white light continuum as the probe.

The time delay between the pump beam and the probe pulses was controlled by a motorized delay stage. The transmitted probe light after sample was collected by a laser frequency synchronized fiber optical spectrometer (AvaSpec-ULS2048CL-EVO, Avantes). When chopping the pump laser beam with half of the laser frequency, the probe light in the case of pump *on*/*off* was acquired and finally the pump pulse induced optical density change of the sample was calculated. During the experiment, the pump intensity was set to be 100 nJ cm^{-2}.

1.8 Transient photocurrent response and HER electrochemical characterization

A working electrode was made by drop casting 100 μL of the Au NSs and Au@Pt NSs with different shell thicknesses to cover an ITO slide (1 cm^2). To characterize the interfacial properties of the electrodes, the photocurrent tests were implemented in Na_2SO_4 aqueous (0.1 M) electrolyte solution and the working electrodes were irradiated by a xenon lamp with a proper distance for a focused incident light intensity. The measurements were carried out with or without illumination at open circuit voltages with 0.4 V (vs Ag/AgCl). LSV curves of Au NSs, Pt NPs and Au@Pt NSs with different shell thicknesses under the PRI *on* and *off* in a 0.5 M H_2SO_4 solution (pH=0.48) and the potential was calibrated to the reversible hydrogen electrode (RHE) for the tests of HER (the potential of the Ag/AgCl is 0.197 vs. RHE).

2. Figures and Tables

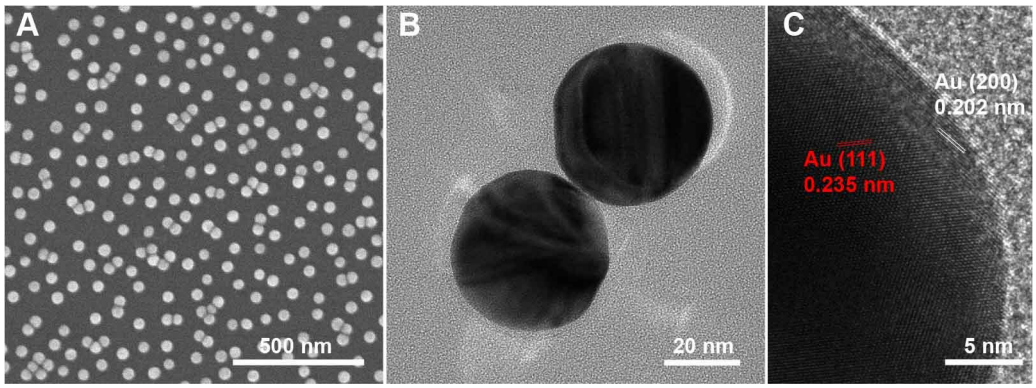

Fig. S1 Characterizations of Au NSs. SEM (A), TEM (B) and HRTEM (C) images of Au NSs.

The as-obtained Au NSs were uniform spherical shapes and had smooth surfaces (Figure S1A and 1B), and their clear fringe of 0.202 and 0.235 nm should be ascribed to the face-centered cubic (*fcc*) Au (200) and (111) lattice planes, respectively (Figure S1C).[2]

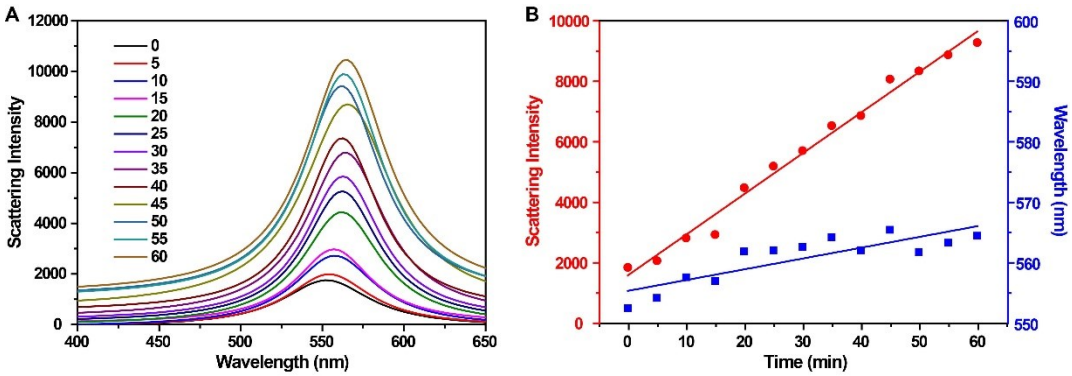

Fig. S2 Real time monitoring the e^{-}_{ph}-reduction by PRLS spectroscopy. (A) PRLS spectra fitted by Lorentz of an individual Au NS; (B) λ_{max} (blue dots) and intensity (red dots) of PRLS change as a function of reduction times. The λ_{max} was red-shifted from 552 nm to 566 nm and the intensity dramatically got increased nearly 5 times.

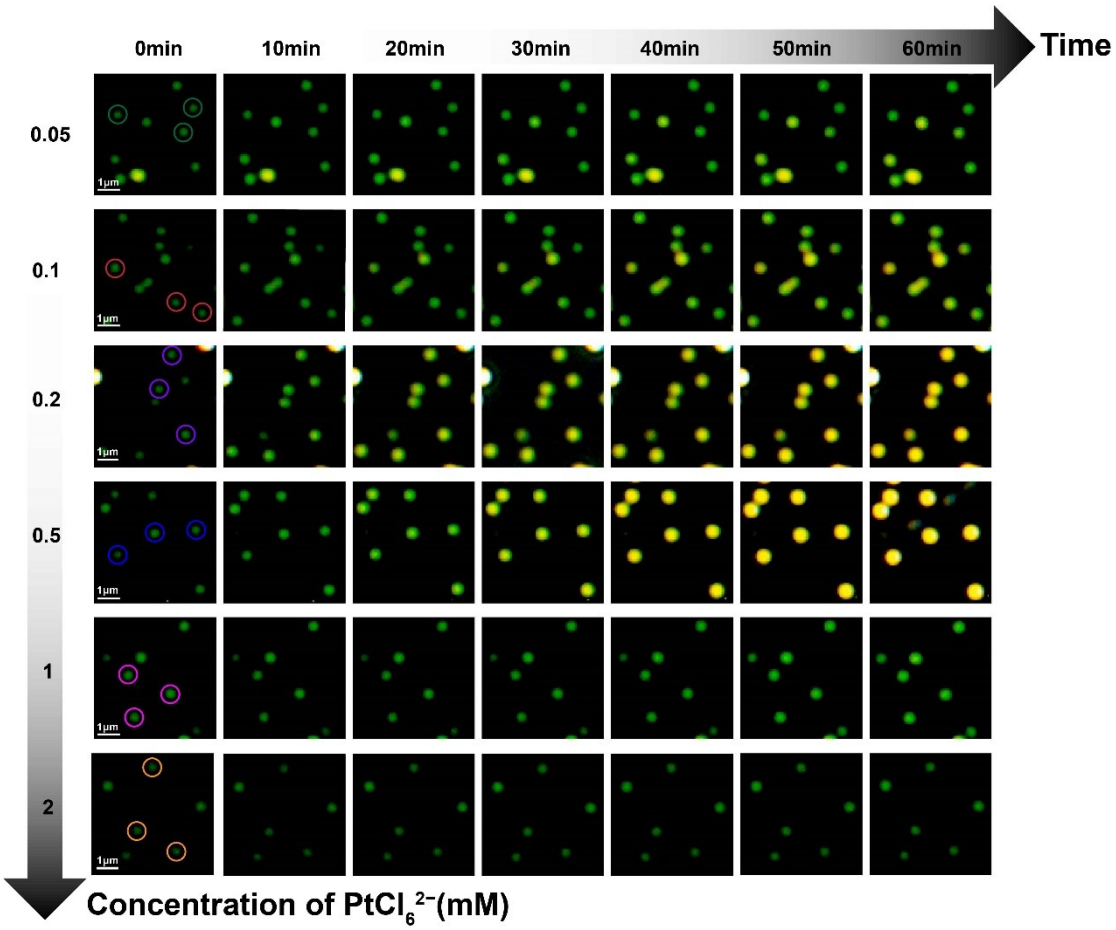

Fig. S3 The time-dependent PRLS images of Au NSs with different concentration of H_2PtCl_6.

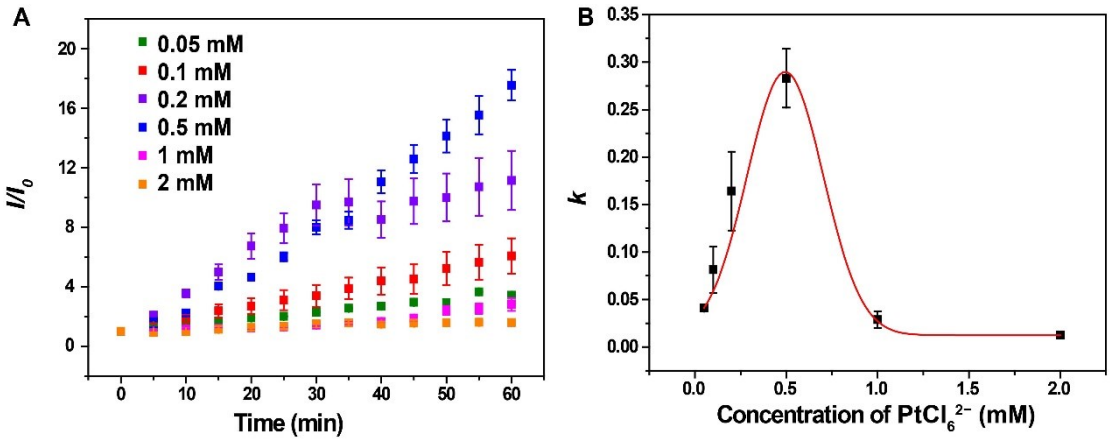

Fig. S4 (A) Time dependent PRLS intensity evolution and (B) the fitted rate constants of the Au NSs with different concentration of H_2PtCl_6. Error bars are calculated from these circled particles (n=3).

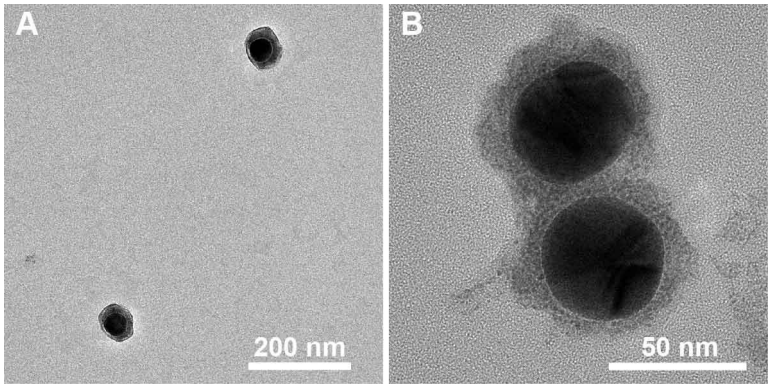

Fig. S5 Characterizations of Au@Pt NSs after 30 min plasmonic resonance illumination (PRI). (A and B) TEM images with different scale bar.

The as-obtained nanostructures (Au@Pt NSs) displayed apparent core-shell structures due to the clear difference in atomic number and thus attenuation of electrons.

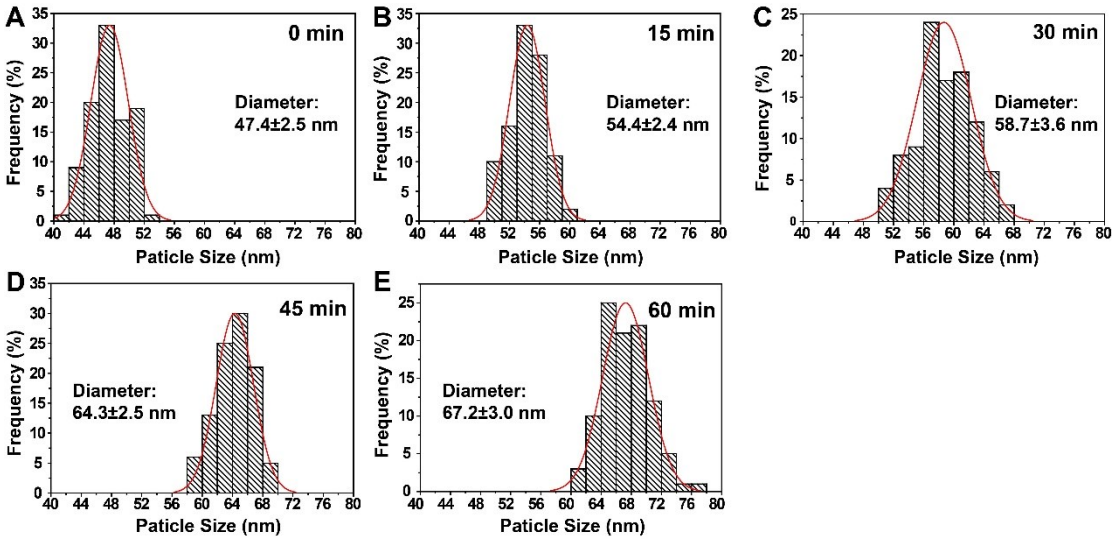

Fig. S6 (A-E) Size distribution histograms of Au@Pt NSs taken at every 15 min interval to monitor the e_{ph}^{-} reduction of the Pt shell under PRI over 60 min reaction. The size of the particles was generally increased along with the PRI time, which varied from 47.4 ± 2.5 nm, 54.4 ± 2.4 nm ,58.7 ± 3.6 nm, 64.3 ± 2.5 nm to 67.2 ± 3.0 nm corresponding to the time of 0, 15, 30, 45 and 60 min. The particle size statistics come from 100 particles(n=100).

Calculation of the hot electrons numbers participating the reduction of $PtCl_6^{2-}$.

Volume of Pt shell of an individual Au@Pt NS:

$$V_{Pt\ shell} = V_{Au@Pt\ NS} - V_{Au\ NS} = \frac{4}{3}\pi(R^3_{Au@Pt\ NS} - R^3_{Au\ NS})$$

Number of Pt atoms of an individual Au@Pt NS (N_{Pt}):

$$N_{Pt} = \frac{m_{Pt\ shell}}{M_{Pt}}N_A = \frac{V_{Pt\ shell}\,\rho_{Pt}}{M_{Pt}}N_A = \frac{\frac{4}{3}\pi(R^3_{Au@Pt\ NS} - R^3_{Au\ NS})\,\rho_{Pt}}{M_{Pt}}N_A$$

Number of electrons obtained by an individual Au@Pt NS (N_e) owing to the four electrons transfer from $PtCl_6^{2-}$ ions to form Au@Pt NSs:

$$N_e = 4N_{Pt} = \frac{16\pi(R^3_{Au@Pt\ NS} - R^3_{Au\ NS})\,\rho_{Pt}}{3M_{Pt}}N_A$$

Table S1. Comparison of Au@Pt NSs growth under different PRI time.

PRI Time (min)	0	15	30	45	60
I/I_0	1.0	2.5	5.1	8.1	11.8
Diameter of particles (nm)	47.4	54.4	58.7	64.3	67.2
Shell thickness of Pt (nm)	0	7.0	11.3	16.9	19.8
$\boldsymbol{V}_{\mathbf{Pt\ shell}}$ (nm^3)	0	28517.8	50117.3	89393.8	103079.9
$\boldsymbol{N}_{\mathbf{Pt}}$ (10^9)	0	1.9	3.3	5.5	6.8
$\boldsymbol{N}_{\mathbf{e}}$ (10^{10})	0	0.76	1.3	2.2	2.7

ρ_{Pt}=21.45g/cm^3

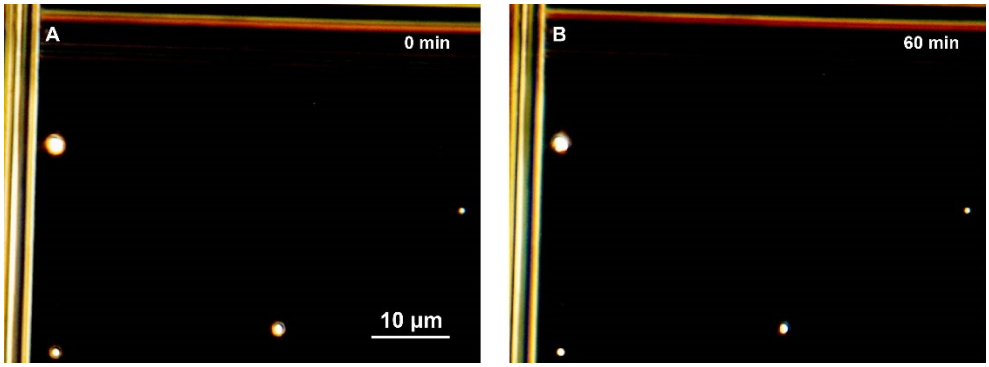

Fig. S7 Control experiment showing the critical role of Au NSs in terms of plasmonic resonance that generates e^-_{ph} under PRI. PRLS images collected in the same observation window before (A) and after (B) the PRI for 60 min.

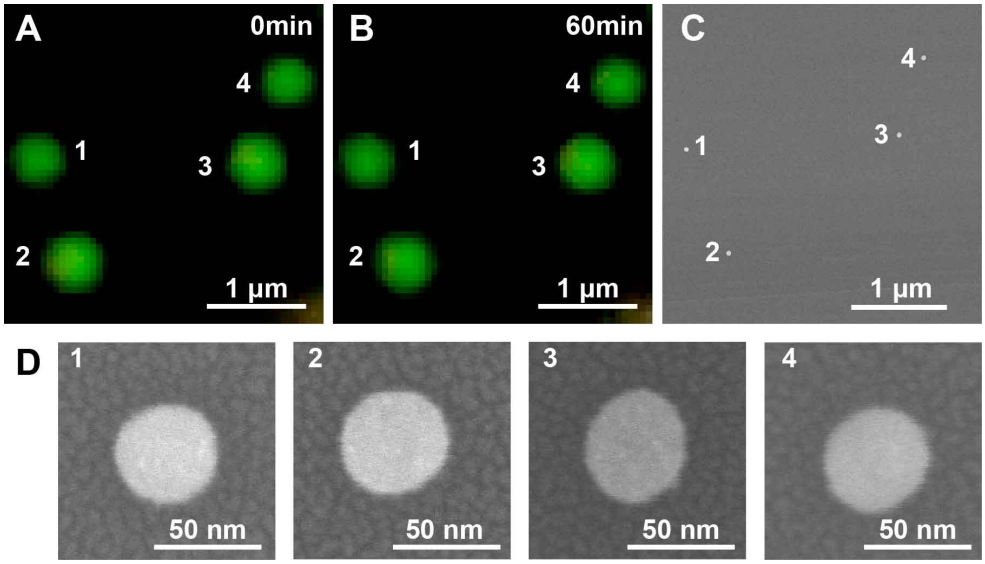

Fig. S8 Control experiment showing the critical role of $PtCl_6^{2-}$ in the e^-_{ph}-reduction. PRLS images of the Au NSs collected in the same observation window before (A) and after (B) the PRI for 60 min without $PtCl_6^{2-}$. (C) The corresponding SEM images shown in B; (D) The enlarged SEM images of these corresponding Au NSs.

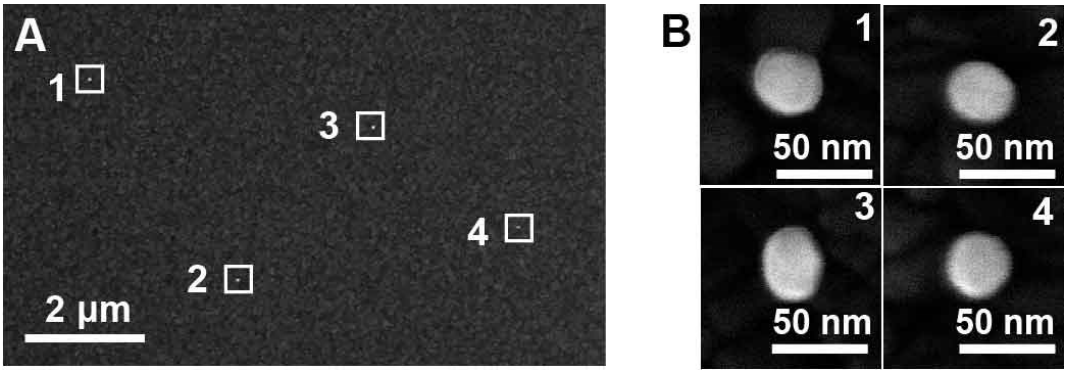

Fig. S9 Control experiment in terms of the importance of PRI conducted in the dark for 60 min. (A) The corresponding SEM images shown in Figure 3A; (B) The enlarged SEM images of these corresponding Au NSs.

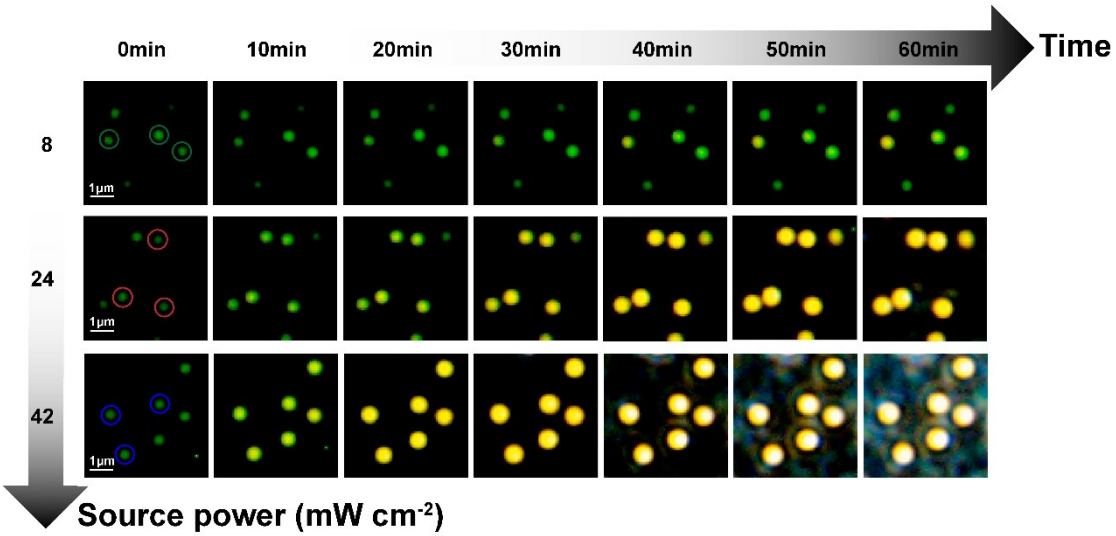

Fig. S10 The influence of source power in the e_{ph}^{-}-reduction. The time-dependent PRLS images of Au NSs under PRI with different source power.

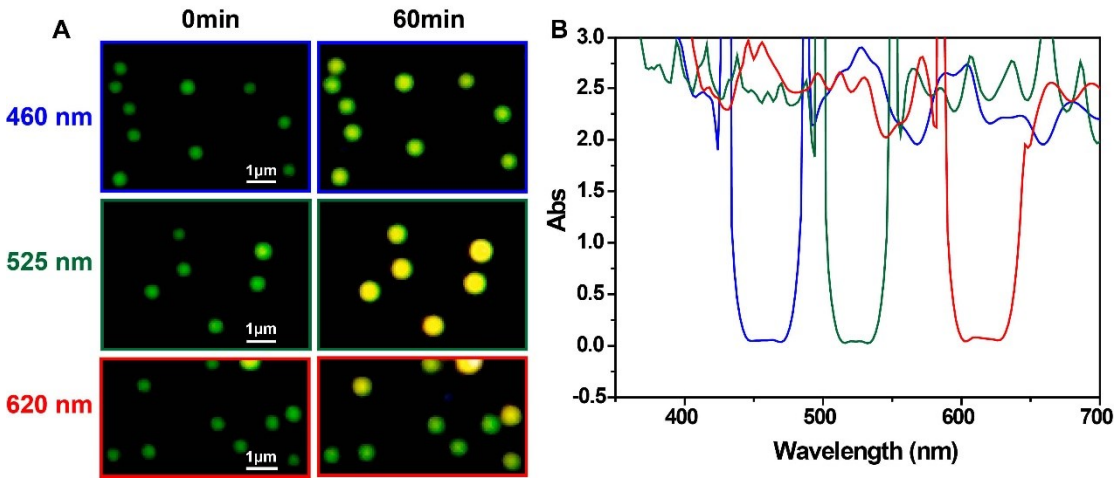

Fig. S11 Influence of illumination wavelength in the e^{-}_{ph}-reduction. (A) PRLS images collected in the same observation window before and after 60 min of illumination with various excitation wavelengths (Top to down: 460 nm, 525 nm and 620 nm, respectively). (B) UV-vis absorption spectra of different pass filter (blue curve: 460±15 nm; green curve: 525±10 nm and red curve: 620±15 nm, respectively).

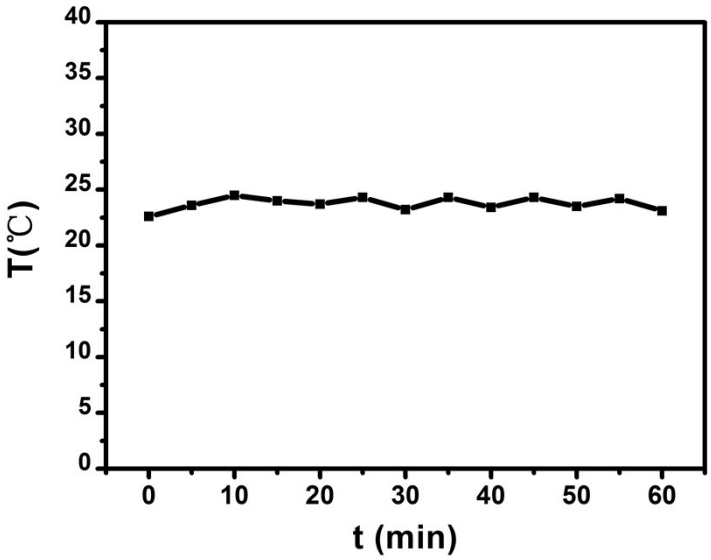

Fig. S12 Photothermal effect of Au NSs incubated in the $PtCl_6^{2-}$ solution with halogen lamp.

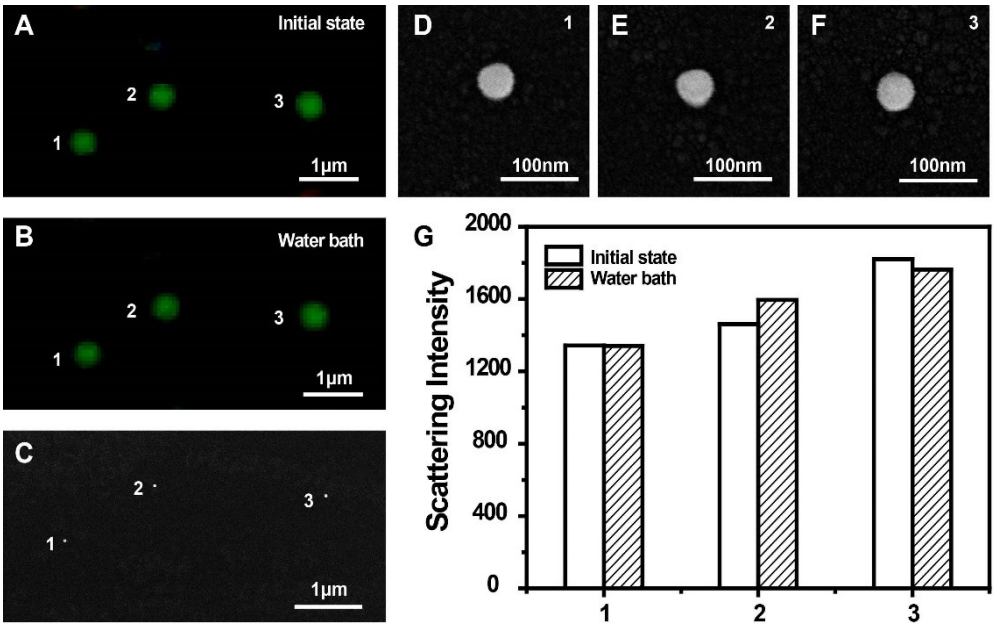

Fig. S13 Photothermal control experiment conducted in the dark at 37 ^{o}C for 60 min. PRLS images collected in the same observation window in initial state (A) and after water bath (B) for 60 min; (C) The corresponding SEM images shown in B; (D-F) The enlarged SEM images of the corresponding particles; (G) The corresponding changes of PRLS intensity of the corresponding particles.

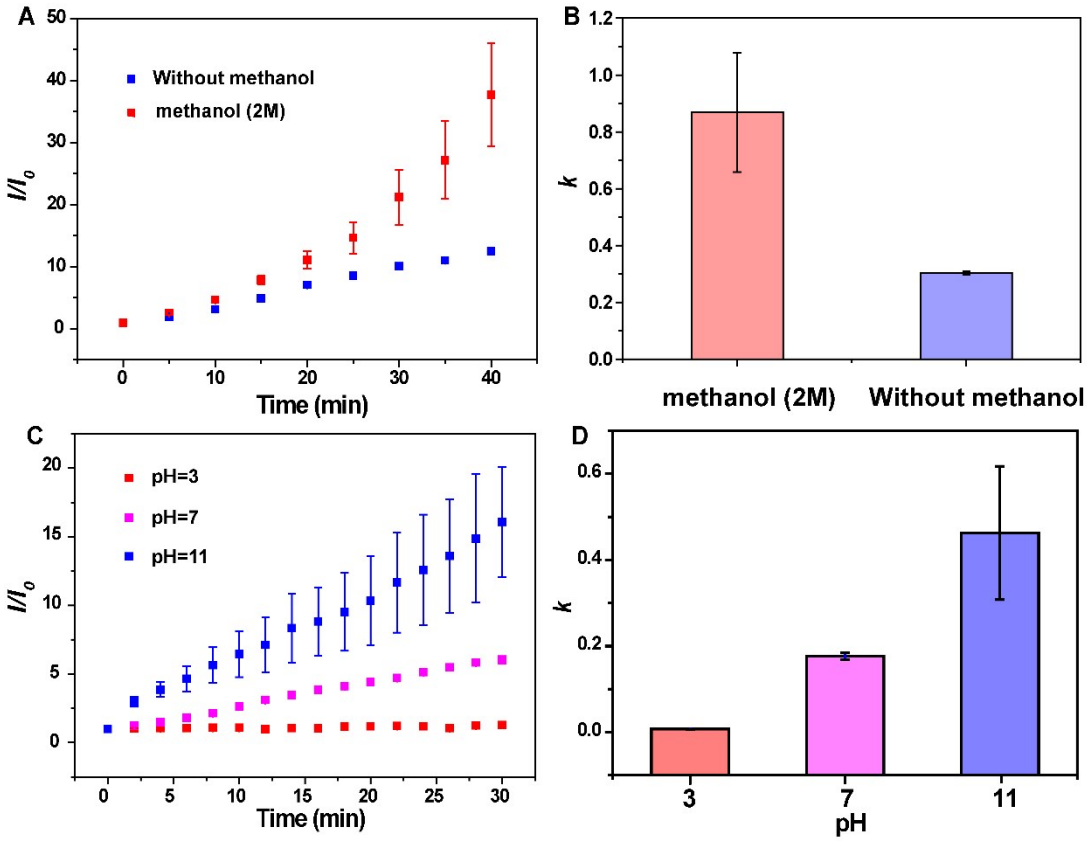

Fig. S14 The influence of hole scavengers in the $^{e}_{ph}$-reduction. (A) PRLS intensity evolution and (B) the fitted rate constants of Au NSs (the circled particles in Figure S15) without and with 2M methanol as hole scavenger. Error bars are calculated from these circled particles (n=3). (C) PRLS intensity evolution and (D) the fitted rate constants of Au NSs (the circled particles in Figure S16) with different pH values. Error bars are calculated from there circled particles (n=3).

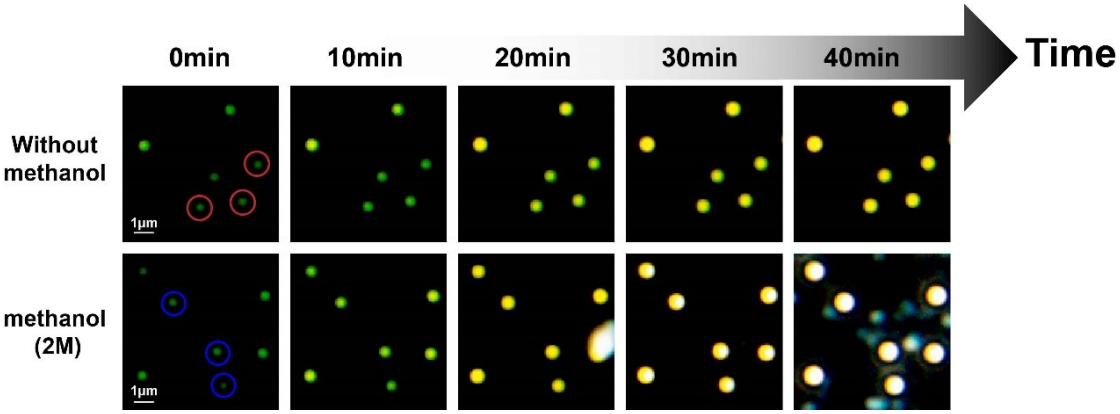

Fig. S15 The time-dependent PRLS images of Au NSs without and with 2M methanol as hole scavenger.

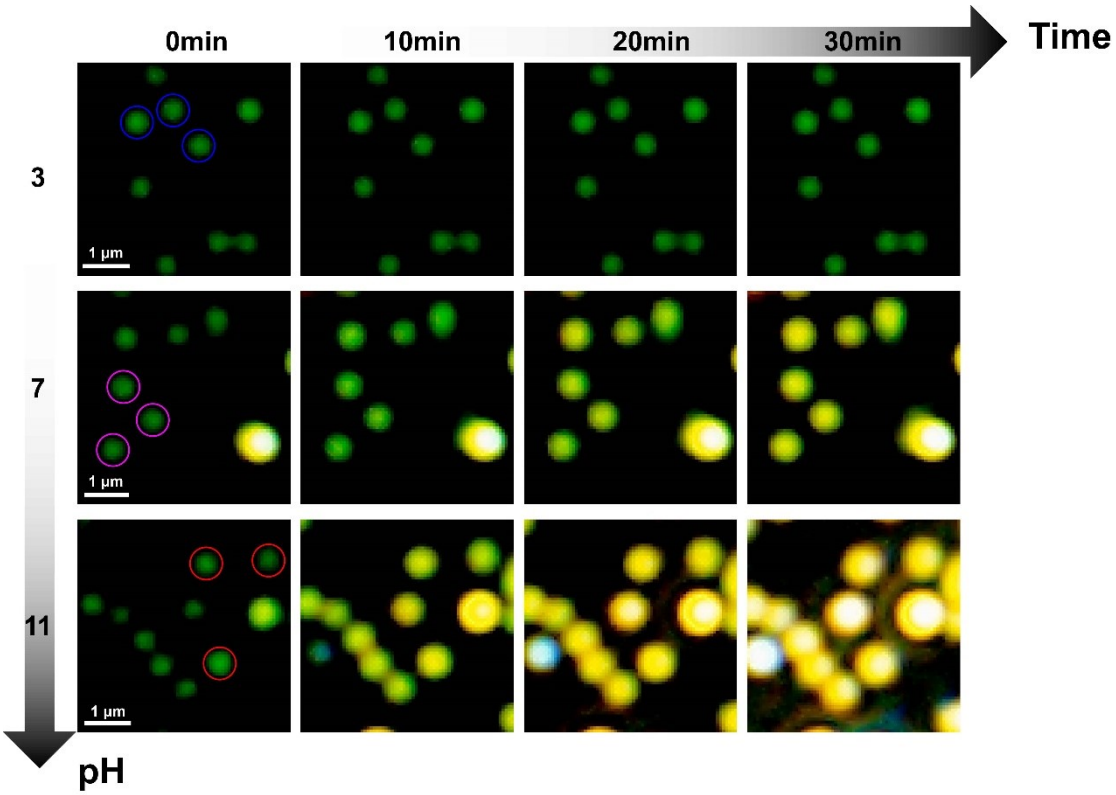

Fig. S16 The time-dependent PRLS images of Au NSs with different pH values.

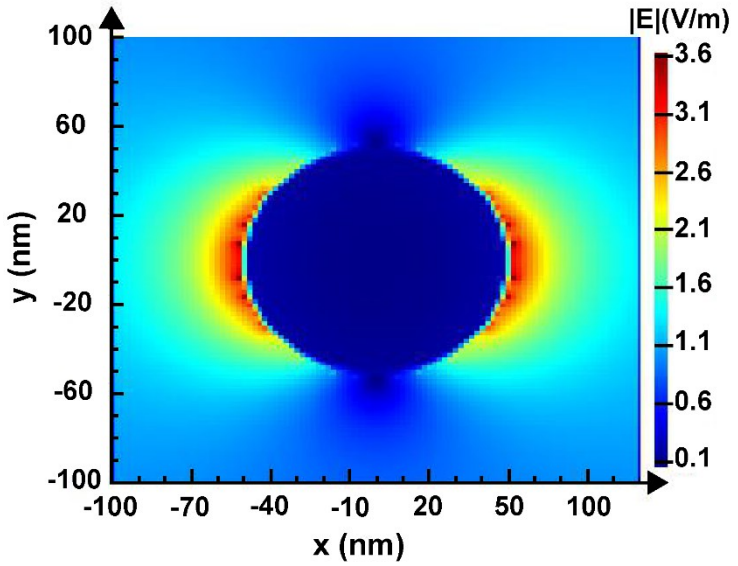

Fig. S17 Electric field distribution around 47 nm Au NS.

References

1 Q. Ruan, L. Shao, Y. Shu, J. Wang and H. Wu, *Adv. Optic. Mater*, 2014, **2**, 65-73.

2 H. Wang, W. Zhao, C.-H. Xu, H.-Y. Chen and J.-J. Xu, *Chem. Sci.*, 2019, **10**, 9308-9314.